Inorg. Chem. **2008**, *47*, 9886−9897

Inorganic Chemistry
Article

Formation of P−C Bonds under Unexpectedly Mild Conditions. Phosphoryl Migration and Metal Coordination of Diphenylphosphinomethyl-oxazolines and -thiazolines

Roberto Pattacini, Günter Margraf, Abdelatif Messaoudi, Nicola Oberbeckmann-Winter, and Pierre Braunstein*

Laboratoire de Chimie de Coordination, Institut de Chimie (UMR 7177 CNRS), Université Louis Pasteur, 4 rue Blaise Pascal, F-67070 Strasbourg Cedex, France, Fax: (+33) (0)3 90 24 13 22

Received May 22, 2008

The heterocycles 2-methyl-2-oxazoline (mox) and 2-methyl-2-thiazoline (mth) react with Ph_2PCl under mild conditions, in the presence of NEt_3 which promotes their phosphorylation by stabilization of their enamino tautomers mox_e and mth_e, respectively, and which also behaves as HCl scavenger. Depending on the reaction conditions, three different phosphine ligands were obtained in good yields from mox: the monophosphine $Ph_2PCH_2C{=}NCH_2CH_2O$ (**1**$_{ox}$) and the isomeric diphosphines $Ph_2PCH{=}COCH_2CH_2NPPh_2$ (**2**$_{ox}$) (X-ray structure) and $(Ph_2P)_2CHC{=}NCH_2CH_2O$ (**3**$_{ox}$). The formation of these ligands involves phosphoryl migration reactions, which were studied by NMR spectroscopy. The synthesis and the X-ray structures of the corresponding diphenylphosphinothiazolines $Ph_2PCH_2C{=}NCH_2CH_2S$ (**1**$_{th}$) and $Ph_2CH{=}CSCH_2CH_2NPPh_2$ (**2**$_{th}$) are also reported but the thiazoline analog of the geminal diphosphine **3**$_{ox}$ was not observed. The metal complexes $[Pt(\mathbf{3}_{ox\text{-}H})_2]\cdot 4CH_2Cl_2$ (**4**$\cdot 4CH_2Cl_2$), $[Pt(Me)I(\mathbf{1}_{ox})]$ (**5**), $[Pt(Me)_2(\mathbf{1}_{ox})]$ (**7**), $[Pd(dmba\text{-}C,N)(\mathbf{1}_{th})]OTf\cdot 0.25Et_2O$ (**8**$\cdot 0.25Et_2O$), $[Pd(dmba\text{-}C,N)(\mathbf{1}_{th\text{-}H})]$ (**9**), and $[\mathbf{9}\cdot\{Pd(dmba\text{-}C,N)Cl\}]\cdot 2.5C_6H_6$ (**10**$\cdot 2.5C_6H_6$) have been prepared and structurally characterized by X-ray diffraction.

Introduction

The synthesis of chelating *P*,*N* ligands and their applications in coordination chemistry are attracting much attention.[1] The introduction of an alkyl-phosphine moiety in a ligand generally requires delicate reaction conditions (alkyllithium compounds, amide bases at low temperatures), when compared to those used for the preparation of other classes of organophosphorus compounds, such as phosphinites or aminophosphines. In the latter cases, chlorophosphines (e.g., Ph_2PCl) are generally reacted with the parent alcohol or amine, respectively, in a one step reaction involving the use of NEt_3 as HCl scavenger. Although such reactions usually simply involve a H/PPh_2 exchange, a nontrivial reaction pathway was recently discovered for the reaction of Ph_2PCl with 2-amino-2-thiazoline in the presence of NEt_3, as depicted in Scheme 1.[2]

Scheme 1

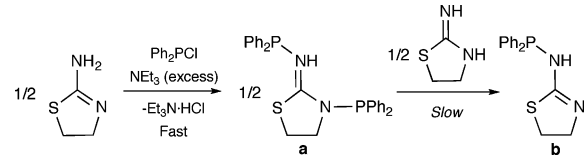

This reaction proceeds by fast double phosphorylation of 2-amino-2-thiazoline, leading first to diphosphine **a**, which then reacts more slowly with the imino-form of the 2-amino-

* To whom correspondence should be addressed. E-mail: braunstein@chimie.u-strasbg.fr.

(1) For example, see: (a) Benito-Garagorri, D.; Kirchner, K. *Acc. Chem. Res.* **2008**, *41*, 201–213. (b) Roseblade, S. J.; Pfaltz, A. *Acc. Chem. Res.* **2007**, *40*, 1402–1411. (c) Braunstein, P. *Chem. Rev.* **2006**, *106*, 134–159. (d) Braunstein, P. *J. Organomet. Chem.* **2004**, *689*, 3953–3967. (e) Guiry, P. J.; Saunders, C. P. *Adv. Synth. Catal.* **2004**, *346*, 497–537. (f) Chelucci, G.; Orru, G.; Pinna, G. A. *Tetrahedron* **2003**, *59*, 9471–9515. (g) Pfaltz, A.; Blankenstein, J.; Hilgraf, R.; Hormann, E.; McIntyre, S.; Menges, F.; Schonleber, M.; Smidt, S. P.; Wustenberg, B.; Zimmermann, N. *Adv. Synth. Catal.* **2003**, *345*, 33–44. (h) Braunstein, P.; Naud, F. *Angew. Chem., Int. Ed.* **2001**, *40*, 680–699. (i) Helmchen, G.; Pfaltz, A. *Acc. Chem. Res.* **2000**, *33*, 336–345. (j) Slone, C. S.; Weinberger, D. A.; Mirkin, C. A. *Prog. Inorg. Chem.* **1999**, *48*, 233–350. (k) Espinet, P.; Soulantica, K. *Coord. Chem. Rev.* **1999**, *193*−*195*, 499–556.

(2) Margraf, G.; Pattacini, R.; Messaoudi, A.; Braunstein, P. *Chem. Commun.* **2006**, 3098–3100.

10.1021/ic800934h CCC: $40.75
Published on Web 10/03/2008

2-thiazoline, to yield the monophosphine **b** as the final product. The reaction is under kinetic control, with the attack of Ph_2PCl on 2-amino-2-thiazoline to give **a** being significantly faster than the **a** → **b** transformation.

We became interested in investigating whether these mild reaction conditions could be applied to isoelectronic, mixed alkyl-aryl phosphines (2-oxazoline-2-ylmethyl)diphenylphosphine ($\mathbf{1_{ox}}$) and (2-thiazoline-2-ylmethyl)diphenylphosphine ($\mathbf{1_{th}}$).

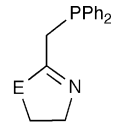

E = O ($\mathbf{1_{ox}}$)
E = S ($\mathbf{1_{th}}$)

The former ligand[3] and its substituted derivatives[4] have been successfully applied in several catalytic processes and are usually obtained by multistep reactions involving (i) lithiation of 2-methyl-2-oxazoline (mox), usually with *n*-BuLi as a base, (ii) silylation with Me_3SiCl, and (iii) phosphorylation with Ph_2PCl. This protocol has been recently followed for the preparation of $\mathbf{1_{th}}$.[5] The corresponding mononuclear square-planar Ni(II) complexes $[NiCl_2(L)]$ (L = $\mathbf{1_{ox}}$ or $\mathbf{1_{th}}$) were found to be in equilibrium with a paramagnetic tetramer, which undergoes in the solid state an irreversible pressure-induced fragmentation into the monomer.[5] We shall see below that $\mathbf{1_{ox}}$ and $\mathbf{1_{th}}$ can be more conveniently synthesized in one-pot reactions from the corresponding substrates and chlorophosphine in the presence of triethylamine at room temperature, following nontrivial pathways that involve stable intermediates. We shall also see that these ligands, as well as their rearrangement products, readily form a number of Pd(II) and Pt(II) complexes which have been structurally characterized by X-ray diffraction.

Experimental Section

General Considerations. All manipulations were carried out under inert dinitrogen atmosphere, using standard Schlenk-line conditions and dried and freshly distilled solvents. Unless otherwise stated, the ^1H, $^{13}C\{^1H\}$, and $^{31}P\{^1H\}$ NMR spectra were recorded on a Bruker Avance 300 instrument at 300.13, 75.47, and 121.49 MHz, respectively, using TMS or H_3PO_4 (85% in D_2O) as external standards, with downfield shifts reported as positive. All NMR spectra were measured at 298 K, unless otherwise specified. The assignment of the signals was made by $^1H,^1H$-COSY, and $^1H,^{13}C$-HMQC experiments. Elemental C, H, and N analyses were performed by the "Service de microanalyses", Université Louis Pasteur, Strasbourg. $[Pd(dmba)(\mu\text{-}Cl)]_2$,[6] $[PtCl_2(NCPh)_2]$,[7] $[PtCl_2(cod)]$,[8] $[PtMe_2(cod)]$,[9] $[PtCl(Me)(cod)]$,[10] and $[PtI(Me)(cod)]$[10] (cod = 1,5 cyclooctadiene) were prepared according to literature procedures. Ph_2PCl and NEt_3 were freshly distilled before use. Other chemicals were commercially available and were used as received.

Preparation of $Ph_2PCH_2C{=}NCH_2CH_2O$ ($\mathbf{1_{ox}}$). To a solution of 2-methyl-2-oxazoline (1.00 mL, 11.7 mmol) in toluene (150 mL) were added NEt_3 (1.62 mL, 11.7 mmol) and pure Ph_2PCl (2.15 mL, 11.7 mmol). The reaction mixture turned cloudy and was stirred for one week at room temperature, whereupon a voluminous white precipitate formed. The solid was removed by filtration, and the filtrate was taken to dryness in vacuo to afford $\mathbf{1_{ox}}$ as a pale yellow paste (2.93 g, 10.81 mmol, 93%). Because of the instability of the reaction intermediate $Ph_2PCH{=}COCH_2CH_2NPPh_2$ ($\mathbf{2_{ox}}$) and the very slow speed of the overall reaction described here, the previously reported method, although featuring a multistep manipulation, is to be preferred for the synthesis of $\mathbf{1_{ox}}$, and it yields the ligand in a more reproducible manner.[3f] The spectroscopic data of $\mathbf{1_{ox}}$ have been reported elsewhere.[3f]

Preparation and Spectroscopic Data for $Ph_2PCH{=}COCH_2CH_2NPPh_2$ ($\mathbf{2_{ox}}$). To a solution of 2-methyl-2-oxazoline (1.00 mL, 11.7 mmol) in toluene (150 mL) were added NEt_3 (8.12 mL, 58.5 mmol) and pure Ph_2PCl (4.30 mL, 22.4 mmol). The reaction mixture turned cloudy and was stirred for 12 h at room temperature, whereupon a voluminous white precipitate formed. The reaction mixture was filtered, and the filtrate was taken to dryness in vacuo at 38 °C (oil bath temperature) to afford a colorless solid that was washed with Et_2O (20 mL). Evaporation of the volatiles afforded $\mathbf{2_{ox}}$ as a colorless solid (3.34 g, 7.4 mmol, 63%). Single crystals of $\mathbf{2_{ox}}$ were obtained by layering pentane on its saturated solution in toluene. In CH_2Cl_2, $\mathbf{2_{ox}}$ was found to spontaneously and quickly isomerize to give $(Ph_2P)_2CHC{=}NCH_2CH_2O$ ($\mathbf{3_{ox}}$). This should be taken into account when manipulating $\mathbf{2_{ox}}$. Exposure of $\mathbf{2_{ox}}$ to alcohols should be avoided because it quantitatively undergoes alcoholysis, with formation of $Ph_2PCH_2C{=}NCH_2CH_2O$ ($\mathbf{1_{ox}}$) and phosphinites. For similar reasons, exposure of $\mathbf{2_{ox}}$ to moisture quickly results in the formation of $\mathbf{1_{ox}}$ and $Ph_2P(O)PPh_2$. ^1H NMR (C_6D_6): δ 3.29 (t, 2H, $^3J_{H-H}$ = 7.2 Hz, NCH_2), 4.24 (t, 2H, $^3J_{H-H}$ = 7.2 Hz, OCH_2), 4.63 (dd, 1H, $^2J_{H-P}$ = 5.3 Hz, $^4J_{H-P}$ = 3.1 Hz, PCH), 7.20−7.55 (m, 20H, aromatic). $^{31}P\{^1H\}$ NMR (C_6D_6): δ −27.1 (s, P_C), 38.4 (s, P_N). The $^{13}C\{^1H\}$ spectrum of $\mathbf{2_{ox}}$ is not reported because under the conditions necessary to record good quality spectra, $\mathbf{2_{ox}}$ was found to rapidly isomerize to $\mathbf{3_{ox}}$. Anal. Calcd for $C_{28}H_{25}NOP_2$ (453.45): C, 74.16; H, 5.56; N, 3.09. Found: C, 73.93; H, 5.50; N, 2.89.

(3) (a) Jie, S.; Agostinho, M.; Kermagoret, A.; Cazin, C. S. J.; Braunstein, P. *Dalton Trans.* **2007**, 4472–4482. (b) Braunstein, P.; Clerc, G.; Morise, X.; Welter, R.; Mantovani, G. *Dalton Trans.* **2003**, 1601–1605. (c) Braunstein, P.; Clerc, G.; Morise, X. *New. J. Chem.* **2003**, *27*, 68–72. (d) Braunstein, P.; Naud, F.; Rettig, S. J. *New. J. Chem.* **2001**, *25*, 32–39. (e) Braunstein, P.; Graiff, C.; Naud, F.; Pfaltz, A.; Tiripicchio, A. *Inorg. Chem.* **2000**, *39*, 4468–4475. (f) Braunstein, P.; Fryzuk, M. D.; Le Dall, M.; Naud, F.; Rettig, S. J.; Speiser, F. *Dalton Trans.* **2000**, 1067–1074.

(4) (a) Schrems, M. G.; Neumann, E.; Pfaltz, A. *Angew. Chem., Int. Ed.* **2007**, *46*, 8274–8276. (b) Speiser, F.; Braunstein, P.; Saussine, L. *Organometallics* **2004**, *23*, 2633–2640. (c) Speiser, F.; Braunstein, P.; Saussine, L.; Welter, R. *Organometallics* **2004**, *23*, 2613–2624. (d) Braunstein, P.; Naud, F.; Graiff, C.; Tiripicchio, A. *Chem. Commun.* **2000**, 897–898. (e) Lloyd-Jones, G. C.; Pfaltz, A. *Z. Naturforsch., B: Chem. Sci.* **1995**, *50*, 361–367. (f) Sprinz, J.; Helmchen, G. *Tetrahedron Lett.* **1993**, *34*, 1769–1772.

(5) Kermagoret, A.; Pattacini, R.; Vasquez, P. C.; Rogez, G.; Welter, R.; Braunstein, P. *Angew. Chem., Int. Ed.* **2007**, *119*, 6558–6561.

(6) Cope, A. C.; Friedrich, E. C. *J. Am. Chem. Soc.* **1968**, *90*, 909.

(7) (a) Hartley, F. R. *The Chemistry of Platinum and Palladium*; Applied Science Publishers: London, 1973. (b) Braunstein, P.; Bender, R.; Jud, J.-M. *Inorg. Synth.* **1989**, *26*, 341–350.

(8) Drew, D.; Doyle, J. R. *Inorg. Synth* **1990**, *28*, 346–349.

(9) Clark, H. C.; Manzer, L. E. *J. Organomet. Chem.* **1973**, *59*, 411–428.

(10) Dekker, G. P. C. M.; Buijs, A.; Elsevier, C. J.; Vrieze, K.; van Leeuwen, P. W. N. M.; Smeets, W. J. J.; Spek, A. L.; Wang, Y. F.; Stam, C. H. *Organometallics* **1992**, *11*, 1937–1948.

Preparation and Spectroscopic Data for $(Ph_2P)_2$-CHC=NCH$_2$CH$_2$O ($\mathbf{3_{ox}}$). Solid $\mathbf{2_{ox}}$ was dissolved in a minimum amount of CH_2Cl_2. The colorless solution was stirred overnight under nitrogen. The volatiles were removed under vacuum, affording $\mathbf{3_{ox}}$ as a colorless oil (NMR yield: 97%). ^{1}H NMR ($CDCl_3$): δ 3.34 (second order t, 2H, simulated $^3J_{H-H}$ = 9.0 Hz, NCH_2), 3.45 (second order t, 2H, simulated $^3J_{H-H}$ = 9.0 Hz, OCH_2), 4.39 (s, 1H, PCH), 7.10−7.70 (m, 10H, aromatic). ^{31}P{^{1}H} NMR ($CDCl_3$): δ −9.25 (s). ^{13}C{^{1}H} NMR ($CDCl_3$): δ 37.9 (t, $^2J_{P-C}$ = 28.3 Hz, PCHP), 54.1 (s, NCH_2), 66.9 (s, OCH_2), 128.0 (virtual triplet, $^{3+5}J_{P-C}$ = 6.7 Hz, *m*-Ph), 128.3 (virtual triplet, $^{3+5}J_{P-C}$ = 7.5 Hz, *m*-Ph), 129.1 (s, *p*-Ph), 129.3 (s, *p*-Ph), 133.9 (virtual triplet, $^{2+4}J_{P-C}$ = 21.5 Hz, *o*-Ph), 134.2 (virtual triplet, $^{2+4}J_{P-C}$ = 22.8 Hz, *o*-Ph), 135.9 (virtual triplet, $^{1+3}J_{P-C}$ = 9.8 Hz, *ipso*-Ph), 136.8 (virtual triplet, $^{1+3}J_{P-C}$ = 8.8 Hz, *ipso*-Ph), 164.9 (t, $^2J_{P-C}$ = 3.5 Hz, C=N). The oily nature of $\mathbf{3_{ox}}$ and its sensitivity toward hydrolysis prevented obtention of satisfactory elemental analyses. Its purity was checked by ^{31}P, ^{1}H, and ^{13}C NMR spectroscopic methods.

Preparation and Spectroscopic Data for Ph_2PCH_2-C=NCH$_2$CH$_2$S ($\mathbf{1_{th}}$). To a solution of 2-methyl-2-thiazoline (0.40 mL, 4.16 mmol) in toluene (100 mL) was added NEt_3 (0.58 mL, 4.16 mmol), and the clear solution was stirred for 5 min. After addition of Ph_2PCl (0.76 mL, 4.16 mmol), the reaction mixture turned cloudy and was further stirred for 1 h at room temperature, whereupon a voluminous white precipitate formed. The mixture was filtered off, and the filtrate was taken to dryness in vacuo. The oily, crude product was dissolved in a minimum amount of toluene, and this solution was added dropwise to stirred, cold pentane to afford a pale yellow powder that was collected by filtration and dried in vacuo to afford $\mathbf{1_{th}}$ (0.950 g, 3.33 mmol, 80%). Single crystals of $\mathbf{1_{th}}$ suitable for X-ray diffraction were obtained upon storing the crude product under N_2. The spectroscopic data of $\mathbf{2_{th}}$ have been published elsewhere.[5] Anal. Calcd for $C_{16}H_{16}NPS$ (285.34): C, 67.35; H, 5.65; N, 4.91. Found: C, 67.27; H, 5.33; N, 4.41.

Preparation and Spectroscopic Data for Ph_2PCH=CSCH$_2$CH$_2$NPPh$_2$ ($\mathbf{2_{th}}$). To a stirred solution of $\mathbf{1_{th}}$ (0.450 g, 1.58 mmol) in THF (10 mL) were added successively NEt_3 (0.22 mL, 1.58 mmol) and Ph_2PCl (0.29 mL, 1.58 mmol), whereupon the initially clear yellow solution turned cloudy. After it was stirred for 1 h at room temperature, the reaction mixture was filtered through a Schlenk frit directly into a Schlenk flask containing cold pentane (200 mL). Ligand $\mathbf{2_{th}}$ was collected in two crops, filtered, and dried in vacuo (0.497 g, 1.06 mmol, 67%). ^{1}H NMR ($CDCl_3$): δ 2.96 (t, 2H, $^3J_{H-H}$ = 6.5 Hz, SCH_2), 3.49 (tdd, 2H, $^3J_{H-H}$ = 6.5 Hz, $^5J_{P-H}$ = 2.4 Hz, $^5J_{H-H}$ = 0.4 Hz, NCH_2), 5.75 (ddt, 1H, $^2J_{P-H}$ = 5.0 or 4.5 Hz, $^4J_{P-H}$ = 4.5 or 5.0 Hz, $^5J_{H-H}$ = 0.4 Hz, simulated, PCH), 7.24−7.47 (m, 20H, aromatic). ^{31}P{^{1}H} NMR ($CDCl_3$): δ −13.2 (s, P_C), 41.4 (s, P_N). Anal. Calcd for $C_{28}H_{25}NP_2S$ (M = 469.52): C, 71.63; H, 5.37; N, 2.98. Found: C, 71.67; H, 5.86; N, 2.42.

Preparation and Spectroscopic Data for [Pt($\mathbf{3_{ox}}$-H)$_2$] (4). Pure NEt_3 (0.30 mL, 2.14 mmol) was added to a solution of freshly prepared $\mathbf{3_{ox}}$ (0.45 g, 1.00 mmol), in dry acetonitrile (20 mL). After addition of $[PtCl_2(NCPh)_2]$ (0.21 g, 0.44 mmol), the reaction mixture was stirred for 3 h, during which the formation of a yellow precipitate was observed. The yellow solid **4** was collected by filtration, washed with MeCN (3 × 5 mL), and dried under vacuum. Complex **4** can be recrystallized by slow evaporation from a saturated 1:1 CH_2Cl_2/hexane solution, affording **4**·4CH_2Cl_2. Single crystals of **4**·4CH_2Cl_2 suitable for X-ray analysis were obtained by layering hexane onto a solution of **4** in CH_2Cl_2 (0.33 g, 0.30 mmol, 68% based on Pt). ^{1}H NMR ($CDCl_3$): δ 3.52 (second order t, 4H, simulated $^3J_{H-H}$ = 8.4, NCH_2), 3.81 (second order t, 4H, simulated $^3J_{H-H}$ = 8.4 Hz, OCH_2), 7.05−7.50 (m, 20H, aromatic). ^{31}P{^{1}H} NMR ($CDCl_3$): δ −33.7 (s, with ^{195}Pt satellites, $^1J_{P-Pt}$ = 1940 Hz). ^{13}C{^{1}H} NMR ($CDCl_3$): δ 31.0 (s, P−C−P), 52.5 (s, br, NCH_2), 66.3 (s, OCH_2), 128.0−133.0 (m, aromatic), 167.7 (s, with ^{195}Pt satellites, $^3J_{C-Pt}$ = 39.4 Hz, *C*=N). Anal. Calcd for $C_{56}H_{48}N_2O_2P_4Pt$ (1099.97): C, 61.15; H, 4.40; N, 2.55. Found: C, 60.89; H, 4.12; N, 2.18.

Preparation and Spectroscopic Data for [PtI(Me)($\mathbf{1_{ox}}$)] (5). To a solution of [PtI(Me)(cod)] (0.150 g, 0.34 mmol) in CH_2Cl_2 (20 mL) was added $\mathbf{1_{ox}}$ (0.091 g, 0.34 mmol), and the mixture was stirred for 2 h. The pale yellow solution turned colorless, and after it was concentrated under reduced pressure, pentane was added to precipitate a colorless powder. The crude product was washed with pentane and dried in vacuo to afford **5** (0.196 g, 0.32 mmol, 95%). Single crystals suitable for X-ray analysis were obtained at room temperature by slow diffusion of heptane into a solution of **5** in toluene. ^{1}H NMR (CD_2Cl_2): δ 0.75 (d, with ^{195}Pt satellites, 3H, $^3J_{H-P}$ = 4.0 Hz, $^2J_{H-Pt}$ = 75.4 Hz, CH_3), 3.29 (dt, with ^{195}Pt satellites, 2H, $^2J_{H-P}$ = 10.1 Hz, $^5J_{H-H}$ = 2.0 Hz, $^3J_{H-Pt}$ = 25.1 Hz, PCH_2), 4.21 (tt, 2H, $^3J_{H-H}$ = 9.7 Hz, $^5J_{H-H}$ = 2.0 Hz, NCH_2), 4.60 (t, 2H, $^3J_{H-H}$ = 9.7 Hz, OCH_2), 7.40−7.79 (m, 10H, aromatic). ^{13}C{^{1}H} NMR ($CDCl_3$): δ −25.0 (d, with ^{195}Pt satellites, $^1J_{C-Pt}$ = 606 Hz, $^2J_{C-P}$ = 5.3 Hz, CH_3), 31.5 (d, with ^{195}Pt satellites, $^2J_{C-Pt}$ = 14.4 Hz, $^1J_{P-C}$ = 38.0 Hz, PCH_2), 56.0 (s, with ^{195}Pt satellites, $^2J_{C-Pt}$ = 15.9 Hz, NCH_2), 73.5 (s, with ^{195}Pt satellites, $^3J_{C-Pt}$ = 12.9 Hz, OCH_2), 128.0−134.0 (m, aromatic, PPh_2), 176.2 (s, with ^{195}Pt satellites, $^2J_{P-C}$ = 14.7 Hz, *C*=N). ^{31}P{^{1}H} NMR ($CDCl_3$): δ 12.0 (s, with ^{195}Pt satellites, $^1J_{P-Pt}$ = 4423 Hz). Anal. Calcd for $C_{17}H_{19}INOPPt$ (606.29): C, 33.68; H, 3.16; N, 2.31. Found: C, 33.31; H, 3.01; N, 2.20.

Preparation and Spectroscopic Data for [PtCl(Me)($\mathbf{1_{ox}}$)] (6). To a solution of [PtCl(Me)(cod)] (0.120 g, 0.340 mmol) in CH_2Cl_2 (20 mL) was added $\mathbf{1_{ox}}$ (0.091 g, 0.34 mmol), and the mixture was stirred for 2 h. The pale yellow solution turned colorless, and after it was concentrated under reduced pressure, pentane was added to precipitate a colorless powder. The crude product was washed with pentane and dried in vacuo to afford **6** (0.160 g, 0.31 mmol, 92%). Single crystals suitable for X-ray analysis were obtained at room temperature by slow diffusion of heptane into a solution of **6** in benzene. ^{1}H NMR (CD_2Cl_2): δ 0.49 (d, with ^{195}Pt satellites, 3H, $^3J_{H-P}$ = 3.2 Hz, $^2J_{H-Pt}$ = 74.1 Hz, CH_3), 3.26 (d, with ^{195}Pt satellites, 2H, $^2J_{H-P}$ = 10.0 Hz, $^3J_{H-Pt}$ = 25.0 Hz, PCH_2), 4.07 (t, 2H, $^3J_{H-H}$ = 9.8 Hz, NCH_2), 4.14 (t, 2H, $^3J_{H-H}$ = 9.8 Hz, OCH_2), 7.40−7.75 (m, 10H, aromatic). ^{13}C{^{1}H} NMR ($CDCl_3$): δ −20.9 (d, with ^{195}Pt satellites, $^2J_{C-P}$ = 6.2 Hz, $^1J_{C-Pt}$ = 639 Hz, CH_3), 31.5 (d, with ^{195}Pt satellites, $^1J_{P-C}$ = 39.6 Hz, $^2J_{C-Pt}$ = 12 Hz, PCH_2), 52.1 (s, with ^{195}Pt satellites, $^2J_{C-Pt}$ = 12 Hz, NCH_2), 72.9 (s, with ^{195}Pt satellites, $^3J_{C-Pt}$ = 11 Hz, OCH_2), 128.0−133.7 (m, aromatic, PPh_2), 175.2 (d, with ^{195}Pt satellites, $^2J_{P-C}$ = 14.3 Hz, $^2J_{P-Pt}$ = 94 Hz, *C*=N). ^{31}P{^{1}H} NMR ($CDCl_3$): δ 13.36 (s, with ^{195}Pt satellites, $^1J_{P-Pt}$ = 4573 Hz). Anal. Calcd for $C_{17}H_{19}ClNOPPt$ (514.84): C, 39.66; H, 3.72; N, 2.72. Found: C, 39.40; H, 3.79; N, 2.65.

Preparation and Spectroscopic Data for [PtMe$_2$($\mathbf{1_{ox}}$)] (7). To a solution of $[PtMe_2(cod)]$ (0.200 g, 0.60 mmol) in CH_2Cl_2 (20 mL) was added $\mathbf{1_{ox}}$ (0.162 g, 0.60 mmol), and the mixture was stirred for 2 h. The pale yellow solution turned colorless, and after it was concentrated under reduced pressure, pentane was added to precipitate a colorless powder. The crude product was washed with pentane and dried in vacuo to afford **7** (0.258 g, 0.522 mmol, 87%).

Single crystals suitable for X-ray analysis were obtained at room temperature by slow diffusion of heptane into a solution of **7** in toluene. ^{1}H NMR (C_6D_6): δ 1.44 (d, with ^{195}Pt satellites, 3H, $^3J_{H-P}$ = 8.2 Hz, $^2J_{H-Pt}$ = 71.0 Hz, *trans*-CH_3-Pt-P), 1.60 (d, with ^{195}Pt satellites, 3H, $^3J_{H-P}$ = 7.5 Hz, $^2J_{H-Pt}$ = 89.3 Hz, *cis*-CH_3-Pt-P), 3.29 (d, 2H, $^2J_{H-P}$ = 8.4 Hz, PCH_2), 3.35 (m, 4H, SCH_2, NCH_2), 6.90−7.69 (m, 10H, aromatic). ^{13}C{^{1}H} NMR (C_6D_6): δ −22.6 (d, with ^{195}Pt satellites, $^1J_{C-Pt}$ = 761 Hz, $^2J_{C-P}$ = 4.9 Hz, *cis*-CH_3-Pt-P), −7.4 (d, with ^{195}Pt satellites, $^1J_{C-Pt}$ = 695 Hz, $^2J_{C-P}$ = 112.8 Hz, *trans*-CH_3-Pt-P), 30.2 (d, $^1J_{P-C}$ = 25.6 Hz, PCH_2), 51.6 (d, with ^{195}Pt satellites, $^3J_{C-P}$ = 2.1 Hz, $^2J_{C-Pt}$ = 24.0 Hz, NCH_2), 70.6 (s, with ^{195}Pt satellites, $^4J_{C-Pt}$ = 12.3 Hz, OCH_2), 127.5−134.0 (m, aromatic, PPh_2), 177.1 (d, $^2J_{P-C}$ = 24.7 Hz, *C*═N). ^{31}P{^{1}H} NMR (C_6D_6): δ 19.6 (s, with ^{195}Pt satellites, $^1J_{P-Pt}$ = 1871 Hz). Anal. Calcd for $C_{18}H_{22}NOPPt$ (494.4): C, 43.73; H, 4.48; N, 2.83. Found: C,43.95; H, 4.40; N, 2.76.

Preparation and Spectroscopic Data for [Pd(dmba-*C*,*N*)-($\mathbf{1_{th}}$)]OTf (8). A solution prepared by addition of solid $AgSO_3CF_3$ (0.643 g, 2.50 mmol) to a solution of [Pd(dmba)(μ-Cl)]$_2$ (0.690 g, 1.25 mmol) in THF (50 mL), was filtered via cannula into a solution of $\mathbf{1_{th}}$ (0.855 g, 3.00 mmol) in THF (30 mL). The yellow solution was stirred overnight at room temperature, whereupon its color changed to orange. The volume of the solution was reduced under vacuum to about 5 mL. The addition of pentane led to the precipitation of an orange solid, which was washed with pentane and dried in vacuo (1.550 g, 2.30 mmol, 92% based on Pd). Single crystals suitable for X-ray analysis were obtained at room temperature by slow diffusion of diethyl ether into a $CHCl_3$ solution of the complex. ^{1}H NMR ($CDCl_3$): δ 2.95 (d, 6H, $^4J_{P-H}$ = 3.0 Hz, $N(CH_3)_2$), 3.65 (t, 2H, $^3J_{H-H}$ = 8.7 Hz, SCH_2), 3.74 (d, 2H, $^2J_{P-H}$ = 11.1 Hz, PCH_2), 4.06 (d, 2H, $^4J_{P-H}$ = 1.8 Hz, NCH_2, dmba), 4.49 (t, 2H, $^3J_{H-H}$ = 8.7 Hz, NCH_2), 6.46−7.04 (m, 4H, aryls, dmba), 7.47−7.79 (m, 10H, aryls, PPh_2). ^{13}C{^{1}H} NMR ($CDCl_3$): δ 35.2 (s, SCH_2), 39.3 (d, $^1J_{P-C}$ = 28.8 Hz, PCH_2), 51.1 (s, $N(CH_3)_2$, dmba), 63.5 (s, NCH_2), 72.6 (d, $^3J_{P-C}$ = 2.6 Hz, NCH_2, dmba), 123.3 (s, aryl, dmba), 125.3 (s, aryl, dmba), 126.2 (d, $^1J_{P-C}$ = 50.8 Hz, *ipso*-aryl), 126.4 (d, J_{P-C} = 6.6 Hz, aryl, dmba), 129.6 (d, $^3J_{P-C}$ = 11.3 Hz, *m*-aryls), 132.6 (d, $^4J_{P-C}$ = 2.4 Hz, *p*-aryls), 133.9 (d, $^2J_{P-C}$ = 12.5 Hz, *o*-aryls), 138.2 (d, J_{P-C} = 13.3 Hz, aryl, dmba), 145.6 (s, C_q-dmba), 148.1 (s, C_q-dmba), 181.5 (d, $^2J_{P-C}$ = 6.8 Hz, *C*═N). ^{19}F{^{1}H} NMR ($CDCl_3$): δ −78.5 (s, SO_3CF_3). ^{31}P{^{1}H} NMR ($CDCl_3$): δ 45.8 (s). Anal. Calcd for $C_{26}H_{28}F_3N_2O_3PPdS_2$ (675.03): C, 46.26; H, 4.18; N, 4.15. Found: C, 46.97; H, 4.45; N, 3.64.

Preparation and Spectroscopic Data for [Pd(dmba-*C*,*N*)-($\mathbf{1_{th\text{-}H}}$)] (9). To a solution of **8** (0.635 g, 0.94 mmol) in THF (100 mL) was added *t*-BuOK (0.267 g, 2.38 mmol), and the mixture was stirred overnight. The red-brown solution was filtered, and the filtrate was taken to dryness in vacuo. The resulting solid was extracted with toluene. The extract was concentrated under vacuum, and pentane was added to precipitate a beige powder (0.482 g, 0.92 mmol, 97.7%). Single crystals suitable for X-ray analysis were obtained at room temperature by slow diffusion of heptane into a benzene solution of **9**. ^{1}H NMR (CD_2Cl_2): δ 2.84 (d, 6H, $^4J_{P-H}$ = 3.6 Hz, $N(CH_3)_2$, dmba), 3.34 (t, 2H, $^3J_{H-H}$ = 6.9 Hz, SCH_2), 3.37 (d, 1H, $^2J_{P-H}$ = 3.6 Hz, PCH), 3.97 (t, 2H, $^3J_{H-H}$ = 6.9 Hz, NCH_2), 3.98 (s, 2H, NCH_2, dmba), 6.61−7.10 (m, 4H, aryl, dmba), 7.34−7.74 (m, 10H, aromatic). ^{1}H NMR (C_6D_6): δ 2.07 (d, 6H, $^4J_{P-H}$ = 2.4 Hz, $N(CH_3)_2$), 3.04 (t, 2H, $^3J_{H-H}$ = 6.9 Hz, SCH_2), 3.37 (bs, 2H, NCH_2, dmba), 3.56 (t, 2H, $^3J_{H-H}$ = 6.9 Hz, NCH_2), 3.79 (d, 1H, $^2J_{P-H}$ = 3.9 Hz, PCH), 6.78−7.92 (m, 14H, aryl). ^{13}C{^{1}H} NMR (CD_2Cl_2): δ 34.9 (s, SCH_2), 50.4 (s, $N(CH_3)_2$, dmba), 57.4 (d, $^1J_{P-C}$ = 65.7 Hz, PCH), 59.6 (s, NCH_2), 73.4 (d, $^3J_{P-C}$ = 2.5 Hz, NCH_2, dmba), 122.5 (s, aryl, dmba), 123.6 (s, aryl, dmba), 125.1 (d, J_{P-C} = 5.1 Hz, aryl, dmba), 128.1−133.3 (m, aromatic, PPh_2), 135.6 (d, $^1J_{P-C}$ = 54.0 Hz, *ipso*-aryl), 138.0 (d, J_{P-C} = 10.3 Hz, aryl, dmba), 148.7 (s, C_q-dmba), 150.1 (s, C_q-dmba), 175.0 (d, $^2J_{P-C}$ = 27.9 Hz, CN). ^{13}C{^{1}H} NMR (C_6D_6): δ 34.9 (s, SCH_2), 49.4 (s, $N(CH_3)_2$, dmba), 57.4 (d, $^1J_{P-C}$ = 66.9 Hz, PCH), 59.6 (s, NCH_2), 73.2 (s, NCH_2, dmba), 122.5 (s, aryl, dmba), 123.7 (s, aryl, dmba), 125.5 (d, J_{P-C} = 5.1 Hz, aryl, dmba), 129.3−133.5 (m, aromatic, PPh_2), 135.9 (d, $^1J_{P-C}$ = 54.3 Hz, *ipso*-aryl), 138.4 (d, J_{P-C} = 9.7 Hz, aryl, dmba), 148.4 (s, C_q-dmba), 150.7 (d, J_{P-C} = 2.8 Hz, C_q-dmba), 175.5 (d, $^2J_{P-C}$ = 27.9 Hz, *C*═N). ^{31}P{^{1}H} NMR (CD_2Cl_2): δ 38.1 (s); ^{31}P{^{1}H} NMR (C_6D_6): δ 37.7 (s). Anal. Calcd for $C_{25}H_{27}N_2PPdS$ (524.95): C, 57.20; H, 5.18; N, 5.34. Found: C, 57.51; H, 4.86; N, 5.34.

Preparation and Spectroscopic Data for [9·{Pd(dmba-*C*,*N*)Cl}] (10). To a solution of **10** (0.098 g, 0.187 mmol) in THF (20 mL) was added [Pd(dmba-*C*,*N*)(μ-Cl)]$_2$ (0.051 g, 0.093 mmol), and the mixture was stirred overnight. The red-brown solution turned orange, and after it was concentrated under reduced pressure, pentane was added to precipitate a beige brown powder. The crude product was washed with pentane and dried in vacuo to afford **10** (0.140 g, 0.175 mmol, 93.5%). Single crystals suitable for X-ray analysis were obtained at room temperature by slow diffusion of heptane into a solution of **10** in benzene (NMR tube). ^{1}H NMR (CD_2Cl_2): δ 2.28 (s, 3H, NCH_3, dmba Pd1), 2.46 (s, 3H, NCH_3, dmba Pd1), 2.64 (d, $^4J_{P-H}$ = 1.4 Hz, 3H, NCH_3, dmba Pd2), 3.09 (d, 3H, $^4J_{P-H}$ = 3.1 Hz, NCH_3, dmba Pd2), 3.32−3.47 (m, 6H, $^3J_{H-H}$ = 2.4 Hz, 3 CH_2), 4.05 (m, 2H, CH_2), 4.75 (d, 1H, $^2J_{P-H}$ = 13.0 Hz, PCHPd2), 6.50−7.95 (m, 18H, aryl). ^{31}P{^{1}H} NMR (C_6D_6): δ 56.1 (s). Anal. Calcd for $C_{34}H_{39}ClN_3PPd_2S$ (801.03): C, 50.98; H, 4.91; N, 5.25. Found: C, 49.26; H, 4.92; N, 4.43.

X-ray Data Collection, Structure Solution, and Refinement for All Compounds. Suitable crystals for the X-ray analysis of compounds $\mathbf{1_{th}}$, $\mathbf{2_{ox}}$, $\mathbf{2_{th}}$, **4**·4CH_2Cl_2, **5**, **7**, **8**·0.25$C_4H_{10}O$, **9**, and **10**·2.5C_6H_6 were obtained as described above. The intensity data was collected at 173(2) K on a Kappa CCD diffractometer[11] (graphite-monochromated Mo Kα radiation, λ = 0.71073 Å). Crystallographic and experimental details for the structures are summarized in Tables 1 and 2. The structures were solved by direct methods (SHELXS-97) and refined by full-matrix least-squares procedures (based on F^2, SHELXL-97)[12] with anisotropic thermal parameters for all the non-hydrogen atoms. The hydrogen atoms were introduced into the geometrically calculated positions (SHELXS-97 procedures) and refined *riding* on the corresponding parent atoms. For $\mathbf{2_{ox}}$, a residual difference electron density peak of 2.43 e Å^{-3} was located at ∼1.38 Å from P1. Although the lone pair of P2 gave rise to a well localized electron density peak too, the latter was very weak when compared to that close to P1. The model has therefore been refined as a 0.7/0.3 mixture of $\mathbf{2_{ox}}$ and its monooxide, respectively. An ORTEP plot, also displaying the oxygen ellipsoid is reported in the Supporting Information for this paper. CCDC 687225 ($\mathbf{1_{th}}$), 699172 ($\mathbf{2_{ox}}$), 687226 ($\mathbf{2_{th}}$), 687227 (**4**·4CH_2Cl_2), 687228 (**5**), 687229 (**7**), 687230 (**8**·0.25$C_4H_{10}O$), 687231 (**9**), and 687232 (**10**·2.5C_6H_6) contain the crystallographic data for this paper that can be obtained free of charge from the Cambridge Crystallographic Data Center via www.ccdc.cam.ac.uk/datarequest/cif.

(11) Bruker-Nonius. *Kappa CCD Reference Manual*; Nonius BV: Delft: The Netherlands, 1998.
(12) Sheldrick., M.; *SHELXL-97, Program for Crystal Structure Refinement*; University of Göttingen: Göttingen, Germany, 1997.

Table 1. Data Collection and Refinement Parameters for $\mathbf{1_{th}}$, $\mathbf{2_{th}}$, $\mathbf{4}\cdot 4CH_2Cl_2$, and **5**

compound	$\mathbf{1_{th}}$	$\mathbf{2_{th}}$	$\mathbf{2_{ox}}$	$\mathbf{4}\cdot 4CH_2Cl_2$	**5**
formula	$C_{16}H_{16}NPS$	$C_{28}H_{25}NP_2S$	$C_{28}H_{25}NP_2O$	$C_{56}H_{48}N_2O_2P_4Pt\cdot 4(CH_2Cl_2)$	$C_{17}H_{19}INOPPt$
M_r	285.33	469.49	461.43	1439.64	606.29
cell setting	monoclinic	triclinic	triclinic	triclinic	triclinic
space group	$P2_1/c$	$P\bar{1}$	$P\bar{1}$	$P\bar{1}$	$P\bar{1}$
a (Å)	11.6510(4)	10.0750 (5)	8.712(1)	9.8628(1)	11.7825(4)
b (Å)	8.0670(3)	10.2980 (5)	11.500(1)	12.5690(2)	12.2252(5)
c (Å)	16.3080(7)	12.5970 (9)	12.651(1)	13.3269(2)	12.8954(5)
α (deg)	90	72.097(2)	80.151(6)	75.749(1)	92.310(2)
β (deg)	109.814(2)	77.206(2)	76.242(7)	73.261(1)	94.819(2)
γ (deg)	90	79.831(4)	77.920(5)	74.076(1)	105.997(2)
V (Å^3)	1442.0(1)	1204.49 (12)	1194.0(2)	1496.0(4)	1775.35(12)
Z	4	2	2	1	4
D_x (Mg m^{-3})	1.314	1.295	1.283	1.598	2.268
μ (mm^{-1})	0.32	0.28	0.20	2.85	9.73
cryst size (mm)	0.11 × 0.09 × 0.08	0.12 × 0.1 × 0.08	0.1 × 0.06 × 0.01	0.05 × 0.05 × 0.04	0.04 × 0.04 × 0.03
measured reflns	6126	7581	6272	16 852	21 754
independent reflns	3861	4997	4218	6853	10 312
obsd reflns	2818	2648	2607	6780	7858
R_{int}	0.041	0.057	0.045	0.042	0.053
θ_{max} (deg)	29.2	26.5	25.05	27.5	30.0
$R[F^2 > 2\sigma(F^2)]$	0.062	0.064	0.072	0.026	0.044
$R_w(F^2)$	0.106	0.133	0.130	0.060	0.112
S	1.06	0.98	1.105	1.05	1.08
params	172	289	299	349	399

Table 2. Data Collection and Refinement Parameters for **7**, $\mathbf{8}\cdot 0.25C_4H_{10}O$, **9**, and $\mathbf{10}\cdot 2.5C_6H_6$

compound	**7**	$\mathbf{8}\cdot 0.25C_4H_{10}O$	**9**	$\mathbf{10}\cdot 2.5C_6H_6$
formula	$C_{18}H_{22}NOPPt$	$4(C_{25}H_{28}N_2PPdS)\cdot 4(CF_3O_3S)\cdot C_4H_{10}O$	$C_{25}H_{27}N_2PPdS$	$C_{34}H_{39}ClN_3PPd_2S\cdot 2.5(C_6H_6)$
M_r	494.43	1387.05	524.92	996.23
cell setting	monoclinic	triclinic	triclinic	triclinic
space group	$P2_1$	$P\bar{1}$	$P\bar{1}$	$P\bar{1}$
a (Å)	11.5550(4)	9.6076(1)	9.661(1)	11.3551(1)
b (Å)	12.4293(4)	12.7675(1)	10.901(2)	13.7549(2)
c (Å)	12.1149(5)	25.3804(4)	12.780(2)	16.4871(2)
α (deg)	90	96.3772(4)	111.414(1)	101.481(1)
β (deg)	97.721(2)	92.9540(4)	110.096(1)	104.670(1)
γ (deg)	90	107.7705(7)	90.230(1)	107.821(1)
V (Å^3)	1724.17(11)	2934.37(6)	1163.75(3)	2262.18(5)
Z	4	2	2	2
D_x (Mg m^{-3})	1.905	1.570	1.498	1.463
μ (mm^{-1})	8.23	0.88	0.97	0.97
cryst size (mm)	0.04 × 0.03 × 0.03	0.07 × 0.07 × 0.03	0.05 × 0.05 × 0.05	0.10 × 0.10 × 0.10
measured reflns	13 581	31 900	9969	20 839
independent reflns	9287	12 127	6784	13 105
obsd reflns	8639	9078	6147	9381
R_{int}	0.055	0.045	0.017	0.032
θ_{max} (deg°)	30.0	26.5	30.1	30.0
$R[F^2 > 2\sigma(F^2)]$	0.047	0.045	0.027	0.041
$R_w(F^2)$	0.120	0.140	0.064	0.093
S	1.00	1.07	1.05	1.04
params	401	739	273	518

Computational Details. All calculations were done using the program system TURBOMOLE.[13] If not mentioned explicitly otherwise, we used the DFT method with the Becke−Perdew functional (BP86).[14] The Coulomb terms were treated by the RI-J approximation.[15] For the structure optimizations, we used SV(P) basis sets[16] (single-ζ for core orbitals, double-ζ for the valence shells and one set of polarization functions for all centers except hydrogen). Single-point energies were calculated with larger triple-ζ valence plus polarization basis sets (TZVP).[17] The Cartesian coordinates of the optimized models and the total energies, computed with BP86/SV(P) and BP86/TZVP methods/bases are reported in the Supporting Information. The absolute and relative energies correspond to the most stable conformations.

Results and Discussion

Ligand Synthesis. In an attempt to develop simple access to the phosphine ligand $Ph_2PCH_2C{=}NCH_2CH_2O$ ($\mathbf{1_{ox}}$) and its analogous thiazoline derivative $Ph_2PCH_2C{=}NCH_2CH_2S$ ($\mathbf{1_{th}}$), mox, and 2-methyl-2-thiazoline (mth) were reacted in toluene with Ph_2PCl in the presence of NEt_3. The products of these reactions are depicted in Scheme 2.

Surprisingly, even when mox and Ph_2PCl were reacted in a 1:1 ratio, in the presence of NEt_3, the diphosphine ligand $Ph_2PCH{=}COCH_2CH_2NPPh_2$ ($\mathbf{2_{ox}}$) was observed as the major

(13) Ahlrichs, R.; Bär, M.; Häser, M.; Horn, H.; Kölmel, C. *Chem. Phys. Lett.* **1989**, *162*, 165–169.
(14) Becke, A. D. *Phys. Rev.* **1988**, *A38*, 3098–3100.
(15) Eichkorn, K.; Treutler, O.; Ohm, H.; Häser, M.; Ahlrichs, R. *Chem. Phys. Lett.* **1995**, *240*, 283–290.
(16) Schäfer, A.; Horn, H.; Ahlrichs, R. *J. Chem. Phys.* **1992**, *97*, 2571–2577.
(17) Schäfer, A.; Huber, C.; Ahlrichs, R. *J. Chem. Phys.* **1994**, *100*, 5829–5835.
(18) (a) Kondoh, A.; Yorimitsu, H.; Oshima, K. *Org. Lett.* **2007**, *9*, 1383. (b) Morise, X.; Braunstein, P.; Welter, R. *Inorg. Chem.* **2003**, *42*, 7752.

Scheme 2

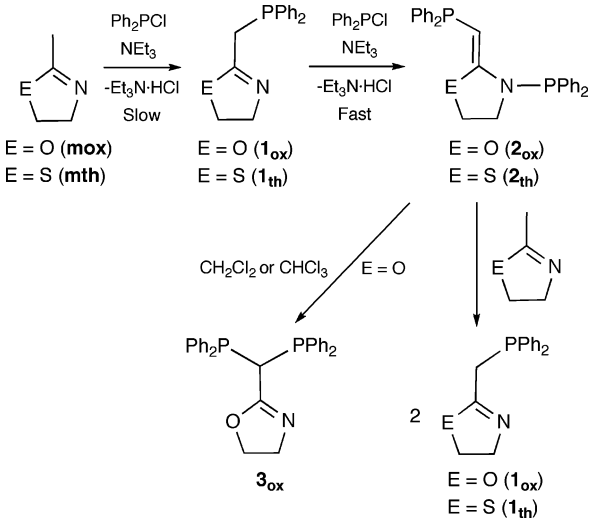

product of the reaction after 12 h reaction time, instead of the expected monophosphine $Ph_2PCH_2C{=}NCH_2CH_2O$ ($\mathbf{1_{ox}}$). This is also the case when a deficiency of Ph_2PCl was used. When the reaction between mox, Ph_2PCl, and NEt_3 was carried out in a 1:1:1 ratio, it proceeded over 1 week to give $\mathbf{1_{ox}}$ in high yield. It was shown independently that diphosphine $\mathbf{2_{ox}}$ slowly reacts with mox to form two molecules of $\mathbf{1_{ox}}$.

When, in the same reaction, Ph_2PCl was added dropwise to a large excess of mox, formation of $\mathbf{2_{ox}}$ and traces of the monophosphine $\mathbf{1_{ox}}$ were observed by in situ $^{31}P\{^1H\}$ NMR spectroscopy, suggesting that under these conditions, the reaction is under kinetic control. The reaction of a second equivalent of Ph_2PCl with $\mathbf{1_{ox}}$ is much faster than the reaction of mox with Ph_2PCl. Similar observations were made with the thiazoline system, although in this case the reaction leading to $\mathbf{2_{th}}$ is faster (vide infra).

Diphosphine $\mathbf{2_{ox}}$ was prepared in good yields by a 2:1 reaction of Ph_2PCl with mox or by reaction of $\mathbf{1_{ox}}$ with Ph_2PCl, under the conditions described above. Ligand $\mathbf{2_{ox}}$ rapidly degrades when exposed to traces of water or alcohols to form $Ph_2P(=O)PPh_2$ and phosphinites, respectively, along with $\mathbf{1_{ox}}$. Moreover, when dissolved in chlorinated solvents such as CH_2Cl_2 or $CHCl_3$, $\mathbf{2_{ox}}$ rapidly isomerizes to the geminal diphosphine $\mathbf{3_{ox}}$.

The reaction of mth with Ph_2PCl proceeds similarly to that of mox, although in this case the rearrangement leading to a geminal diphosphine similar to $\mathbf{3_{ox}}$ was not observed. The crystal structures of $\mathbf{2_{ox}}$, $\mathbf{2_{th}}$, and $\mathbf{1_{th}}$ have been determined by single-crystal X-ray diffraction (Figures 1−3).

The bonding parameters in these molecules are as expected, with the P2−N1 distances in *anti*-diphosphines $\mathbf{2_{ox}}$ and $\mathbf{2_{th}}$ (1.718(3) and 1.718(2) Å, respectively) being shorter than the P1−C4 ones (P1−C4 1.784(4), 1.771(3), and 1.862(2) Å for $\mathbf{2_{ox}}$, $\mathbf{2_{th}}$, and $\mathbf{1_{th}}$, respectively). This may suggest a contribution of the lone pair on N1 to the bonding with P2. Diphosphines $\mathbf{2_{ox}}$ and $\mathbf{2_{th}}$ adopt slightly different conformations, the P1 atom being closer to the chalcogen in $\mathbf{2_{ox}}$ than in $\mathbf{2_{th}}$ (P1···O1 distance in $\mathbf{2_{ox}}$, 3.023(3) Å; P1···S1 distance in $\mathbf{2_{th}}$, 3.258(1) Å). Moreover, P2 is closer to the hydrogen atom on C4 in $\mathbf{2_{ox}}$ than in $\mathbf{2_{th}}$ (P2−C4 distances, 3.199(5) and 3.015(2) Å for $\mathbf{2_{ox}}$ and $\mathbf{2_{th}}$, respectively). As a consequence, the P2 lone pair of $\mathbf{2_{ox}}$ is deviated outside the C4−C3−N1 plane (C3−N1−P2−C23 torsion angle, 132.2(4)° in $\mathbf{2_{ox}}$ and 177.7(3)° in $\mathbf{2_{th}}$).

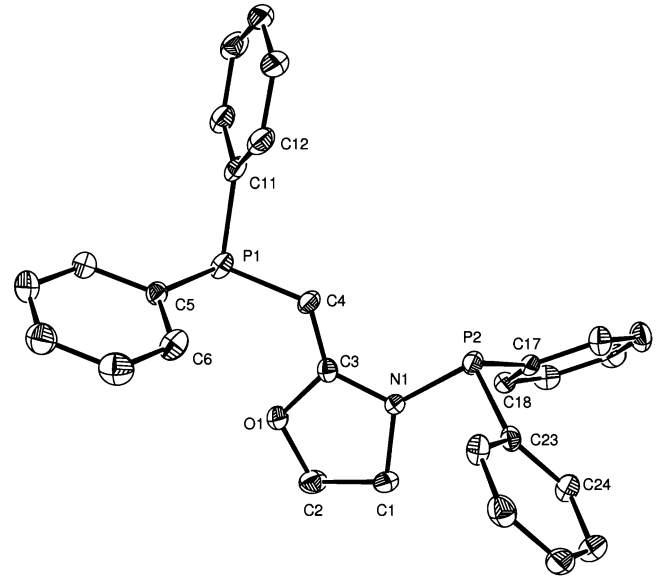

Figure 1. ORTEP plot of the molecular structures of compound $\mathbf{2_{ox}}$. H atoms omitted for clarity. Displacement parameters include 50% of the electron density. Selected bond distances (Å) and angles (deg): N1−C1, 1.472(5); C2−O1, 1.445(5); C3−C4, 1.332(5); N1−C3, 1.391(5); C3−O1, 1.363(4); P1−C4, 1.784(4); P2−N1, 1.718(3); C3−N1−C1, 109.8(3); C3−N1−P2, 122.5(3); C1−N1−P2, 126.1(3); C3−O1−C2, 109.6(3); C(3)−C(4)−P(1), 122.7(3); C(4)−C(3)−O(1), 121.1(3); N(1)−C(3)−C(4), 129.9(4); N(1)−C(3)−O(1), 109.1(3).

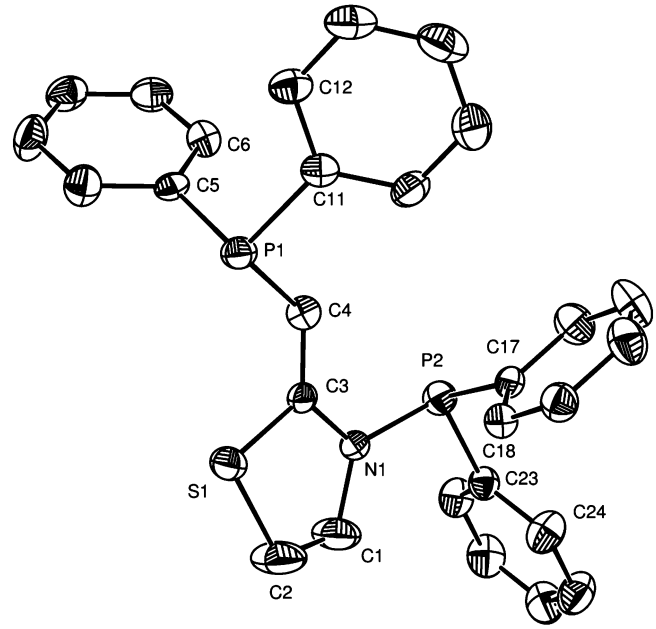

Figure 2. ORTEP plot of the molecular structures of compound $\mathbf{2_{th}}$. H atoms omitted for clarity. Displacement parameters include 50% of the electron density. Selected bond distances (Å) and angles (deg): C(1)−N(1), 1.453(4); C(2)−S(1), 1.770(3); C(3)−C(4), 1.342(4); C(3)−N(1), 1.378(3); C(3)−S(1), 1.749(3); C(4)−P(1), 1.771(3); N(1)−P(2), 1.718(2); C(1)−N(1)−C(3), 114.9(2); C(3)−N(1)−P(2), 117.5(2); C(1)−N(1)−P(2), 126.8(2); C(2)−S(1)−C(3), 92.5(1); C(3)−C(4)−P(1), 122.7(2); C(4)−C(3)−S(1), 123.1(2); N(1)−C(3)−C(4), 126.6(3); N(1)−C(3)−S(1), 110.3(2).

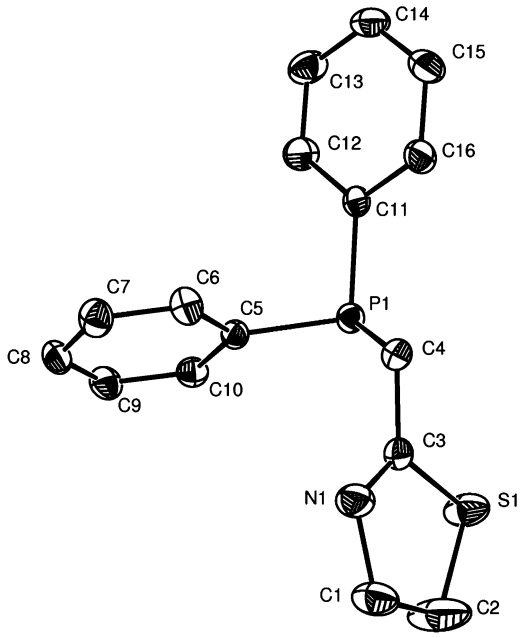

Figure 3. ORTEP plot of the molecular structures of compound $\mathbf{1_{th}}$. H atoms omitted for clarity. Displacement parameters include 50% of the electron density. Selected bond distances (Å) and angles (deg): C(1)−C(2), 1.518(3); C(1)−N(1), 1.469(3); C(2)−S(1), 1.785(3); C(3)−C(4), 1.492(3); C(3)−N(1), 1.264(2); C(3)−S(1), 1.774(2); C(4)−P(1), 1.862(2); C(1)−N(1)−C(3), 112.4(2); C(2)−S(1)−C(3), 90.6(1); C(3)−C(4)−P(1), 112.7(2); C(4)−C(3)−S(1), 117.8(2); N(1)−C(3)−C(4), 124.3(2); (1)−C(3)−S(1), 117.9(2).

These slight geometric differences result, in solution, in dissimilar NMR data. The $^{31}P\{^1H\}$ NMR signal at −27.1 ppm for the Ph_2P-CH=C phosphorus is typical for alkenyl diphenylphosphines,[18] but is upfield shifted when compared to that in $\mathbf{2_{th}}$ (−13.2 ppm). This indicates the influence of the chalcogen, the P1 nucleus of $\mathbf{2_{th}}$ being deshielded because of the different mutal orientation of the lone pairs. Similar steric influences in the chemical shifts of tertiary phosphines were reported for alkenyl phosphines.[19] Moreover, the ^1H NMR spectrum of $\mathbf{2_{th}}$ displays a $^2J(H_{C4},^{31}P)$ coupling constant of 9 Hz, larger than that observed for $\mathbf{2_{ox}}$ (4 Hz).

The reactions mox + 2 Ph_2PCl → $\mathbf{2_{ox}}$ and mth + 2 Ph_2PCl → $\mathbf{2_{th}}$ largely depend on the amount of NEt_3 present in the reaction mixture (e.g., 48 h reaction time for the overall reaction mox + 2 Ph_2PCl → $\mathbf{2_{ox}}$ when performed with a 1:1 Ph_2PCl/NEt_3 ratio vs 1 h with a 1:20 ratio). Direct formation of **1** by a fast H/PPh_2 exchange on a sp^3 carbon, without prior deprotonation, is an unreasonable hypothesis. Two possible alternative mechanisms are proposed in Scheme 3 and discussed below: (a) an electrophilic attack of Ph_2PCl could occur first at the nitrogen, with intermediate formation of the unobserved aminophosphines $\mathbf{i_{ox}}$ and $\mathbf{i_{th}}$, which would then undergo a second attack of the chlorophosphine, to give $\mathbf{2_{ox}}$ and $\mathbf{2_{th}}$, respectively; (b) the enamine forms mox_e and mth_e could be phosphorylated on the exocyclic carbon, forming $\mathbf{1_{ox}}$ and $\mathbf{1_{th}}$, which rapidly react with Ph_2PCl to give the two respective diphosphines.

Mechanism 3a is similar to that proposed for the reaction between mox and acid chlorides ClC(O)R (R = alkyl), which afforded diacyl derivatives of the general formula RC(=O)-CH=COCH$_2$CH$_2$NC(=O)R.[20] Mechanism 3b would imply that NEt_3, prior to HCl scavenging, promotes the presence of the more reactive enamino tautomers of mox and mth (mox_e and mth_e, respectively, Scheme 3). Although mechanism 3a cannot be ruled out, some observations are more in favor of pathway 3b: (i) No reaction was observed between 2-methyl-2-benzoxazole and Ph_2PCl in the presence of NEt_3. In this case, the enamino tautomer is too disfavored by the decreased basicity of the endocyclic nitrogen. (ii) The hypothetical aminophosphines $\mathbf{i_{ox}}$ and $\mathbf{i_{th}}$ were not observed in the reaction mixture. (iii) When mox and Ph_2PCl were stirred in the absence of a base, no trace of cationic aminophosphine was detected. The last step of mechanism 3b was independently achieved, with monophosphines $\mathbf{1_{ox}}$ and $\mathbf{1_{th}}$ rapidly reacting with Ph_2PCl to afford $\mathbf{2_{ox}}$ and $\mathbf{2_{th}}$, respectively. When pyridine was used instead of NEt_3, no reaction was observed. Although pyridine itself is an efficient HCl scavenger, its lower Lewis basicity, when compared to that of NEt_3, is probably not sufficient for the formation of the enamino tautomers in mechanism 3b. However, it may also not be sufficient to achieve the deprotonation step in mechanism 3a.

Because, in the absence of NEt_3, mox and mth do not undergo phosphoryl attack on the exocyclic carbon, it is reasonable to assume that the enamino tautomers mox_e and mth_e are not available in solution under these conditions. As reported in Figure 4 (DFT BP86/TZVP calculations), these tautomers are greatly disfavored with respect to the

Scheme 3

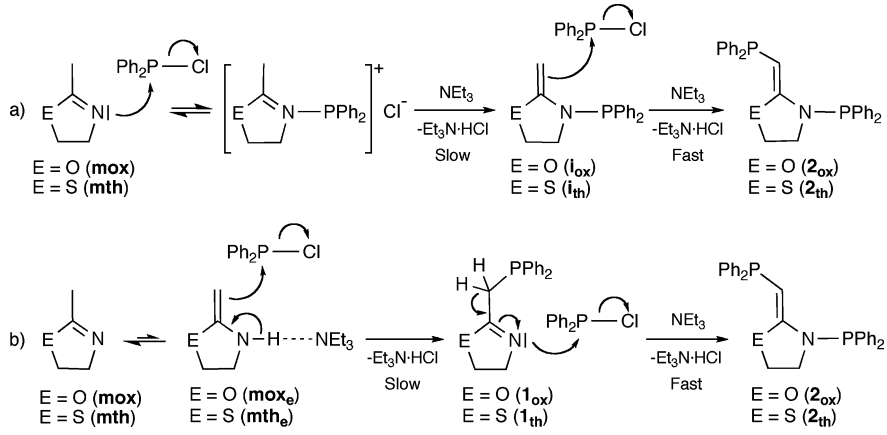

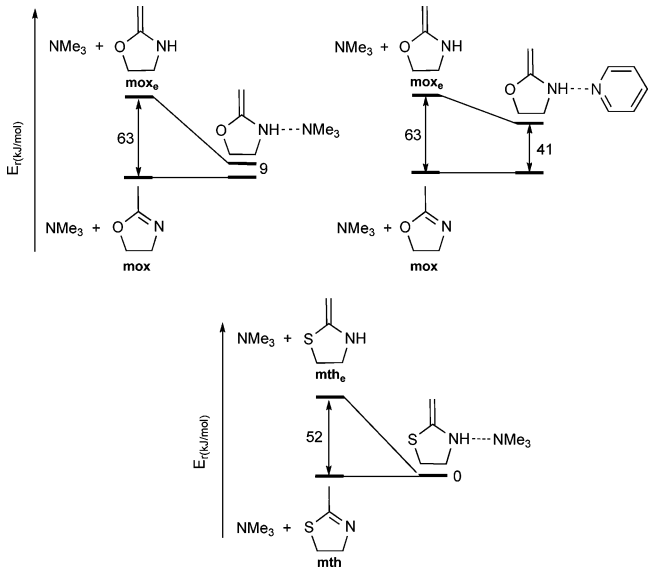

Figure 4. Relative energy diagrams for mox, mox_e, $mox_e \cdot NMe_3$, $mox_e \cdot$pyridine and mth, mth_e, $mth_e \cdot NMe_3$.

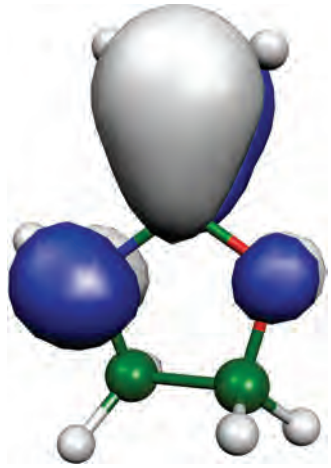

Figure 5. Orbital plot depicting the HOMO of mox_e. In the DFT calculations, NEt_3 was replaced with NMe_3 to avoid issues related to the alkyl chains conformation.

imino forms. However, hydrogen bonding with NEt_3 would make mox_e and mth_e available in solution, because of the significantly decreased energy gap. This gap is significantly larger in the case of pyridine, in agreement with its inability to promote the reaction. These results should be regarded as semiquantitative because the calculations refer to the gas phase and also because of the role played by entropy in the formation of the $Me_3N\cdots$mox complexes. However, the order of magnitude of the stabilization indicates that a trialkylamine can provide the necessary access to the reactive species that undergoes the first phosphorylation. A plot depicting the highest-occupied molecular orbital $2MO_e$ is reported in Figure 5. The HOMO is mainly localized over the $C{=}CH_2$ group and the nitrogen atom, consistent with both mechanisms 3a and 3b.

(19) For example, see: (a) Verkade, J. G.; Quin, L. D. *Phosphorus-31 NMR Spectroscopy in Stereochemical Analysis*; Verlag Chemie: Weinheim, Germany, 1987. (b) Grim, S. O.; Molenda, R. P.; Mitchell, J. D. *J. Org. Chem.* **1980**, *45*, 250–252.

(20) Zhou, A.; Pittman, C. U., Jr. *Tetrahedron Lett.* **2004**, *45*, 8899–8903.

Scheme 4

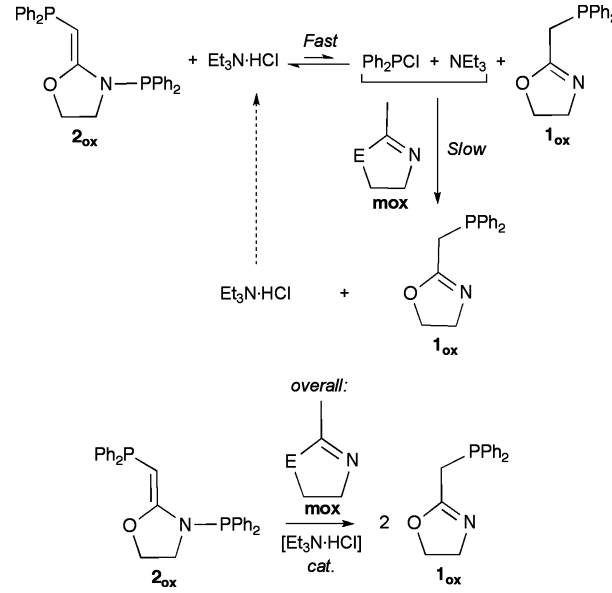

Scheme 5

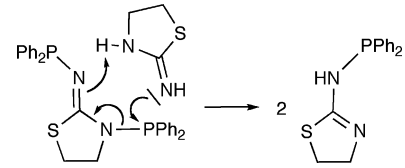

As mentioned above, under certain conditions, $\mathbf{2_{ox}}$ and $\mathbf{2_{th}}$ further react with mox and mth when these are available in solution. However, when the mox + Ph_2PCl + NEt_3 → $\mathbf{2_{ox}}$ reaction was carried out in the presence of a large excess of NEt_3 with respect to Ph_2PCl, formation of $\mathbf{1_{ox}}$ was not observed. Instead, the latter was formed when the base was added in a stoichiometric amount, implying that excess triethylamine inhibits the conversion $\mathbf{2_{ox}}$ + mox → 2 $\mathbf{1_{ox}}$. If NEt_3 is not available in solution, the equilibrium reported in Scheme 4 is established, as demonstrated independently by stirring a suspension of $Et_3N\cdot HCl$ in a solution of $\mathbf{2_{ox}}$ in toluene and in situ $^{31}P\{^1H\}$ NMR monitoring. The resulting diphenylchlorophosphine can, then, attack $\mathbf{1_{ox}}$ (backward reaction) or react with mox, more slowly, although the latter is present in large excess with respect to Ph_2PCl. These two reactions thus compete. Although poorly soluble in toluene, traces of $Et_3N\cdot HCl$ were detected after filtration. This may be the reason for the sensitivity in solution of $\mathbf{2_{ox}}$ toward humidity because of the regeneration of Ph_2PCl. The formation of R_2PCl (R = alkyl, aryl) from aminophosphines and HCl has been described before.[21] The ammonium chloride $Et_3N\cdot HCl$ could then be seen as an HCl carrier, the latter being responsible of the P−N bond cleavage reaction. The ammonium chloride is finally regenerated upon formation of $\mathbf{1_{ox}}$.

The reaction $\mathbf{2_{ox}}$ + mox → $\mathbf{1_{ox}}$ is reminiscent of that observed with 2-amino-2-thiazoline in which the monophosphine $Ph_2PNHC{=}NCH_2CH_2S$ was found to be the thermodynamic product of a multistep reaction, featuring the intermediacy of $Ph_2PN{=}CSCH_2CH_2NPPh_2$ (Scheme 5).[2]

Scheme 6

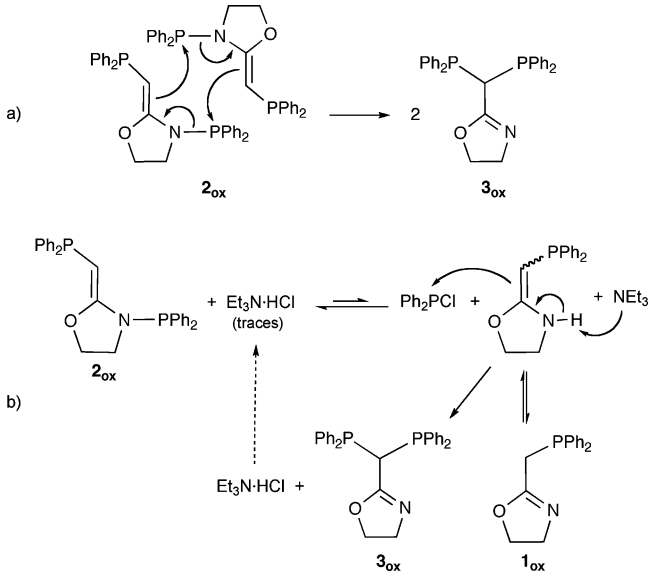

However, at variance with the case reported herein, it was concluded that the diphosphine → monophosphine conversion was the result of a direct intermolecular phosphoryl migration from the exocyclic nitrogen of the diphosphine to the imine of the less stable tautomer of 2-amino-2-thiazole, without the intermediacy of Ph_2PCl (Scheme 5).

The isomerization of $\mathbf{2_{ox}} \rightarrow \mathbf{3_{ox}}$ observed in chlorinated solvents was monitored by $^{31}P\{^1H\}$ NMR and found to be concentration dependent, suggesting an intermolecular mechanism. This reaction is incomplete even after one week under the conditions used for the preparation of $\mathbf{2_{ox}}$, but it is fast in chlorinated solvents (minutes). A concerted mechanism is shown in Scheme 6a, which bears similarities with that in Scheme 5. However, the good solubility of residual $Et_3N{\cdot}HCl$ in chlorinated solvents may facilitate a reaction pathway similar to that of Scheme 3, in which reformed Ph_2PCl may be subject to the nucleophilic attack of the enamino tautomer of $\mathbf{1_{ox}}$ possibly present in solution under these conditions (Scheme 6b). This is currently under study by means of variable temperature NMR and DFT calculations.

The geminal diphosphine $\mathbf{3_{ox}}$ represents a new functionalized dppm ligand,[22] and features similarities with 2-pyridylbis(diphenylphosphino)methane, whose P,N and P,P chelating properties and relevance to homogeneous catalysis have been extensively explored.[23] Formation of $\mathbf{3_{ox}}$ from $\mathbf{1_{ox}}$ and Ph_2PCl in the presence of NEt_3 was not observed in toluene, for two possible reasons: (i) the enamino tautomer of $\mathbf{1_{ox}}$ similar to $\mathbf{mox_e}$ is not available in solution or (ii) under these conditions, attack of the nitrogen atom of $\mathbf{1_{ox}}$ on Ph_2PCl is much faster than that on the carbon α to the phosphorus of the hypothetical enamino tautomer of $\mathbf{1_{ox}}$. Related double phosphorylation reactions leading to functional dppm-type ligands have been observed before but resulted from a different sequence of steps.[24]

Scheme 7

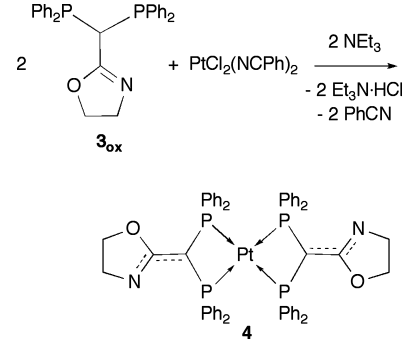

The gas-phase energy profiles reported in Figure 6 were obtained by optimizing several conformers for each ligand, and then choosing those displaying the lower energies. Their Cartesian coordinates are available as Supporting Information. The DFT calculations indicate that in the gas phase the geminal diphosphines $\mathbf{3_{ox}}$ and $\mathbf{3_{th}}$ are slightly disfavored with respect to the parent C,N diphosphines, but this energy gap is smaller for $\mathbf{3_{ox}}$ than for $\mathbf{3_{th}}$, which is consistent with a destabilizing steric effect of the sulfur atom. In solution, this small 5 kJ/mol $\mathbf{2_{ox}}/\mathbf{3_{ox}}$ gap may be readily overcome, allowing the formation of the geminal diphosphine. As mentioned before, the solvent plays indeed an important role in the $\mathbf{2_{ox}} \rightarrow \mathbf{3_{ox}}$ rearrangement.

Metal Complexation. Preliminary attempts to obtain Pt(II) or Pd(II) complexes featuring $\mathbf{2_{ox}}$ as ligand were unsuccessful. Only species containing chelating $\mathbf{1_{ox}}$ (vide infra) were detected in the crude reaction mixtures. Their stability and the lability of the P−N bond in $\mathbf{2_{ox}}$ are probably the reasons for this reactivity pattern.

The reaction of diphosphine $\mathbf{3_{ox}}$ with $[PtCl_2(NCPh)_2]$ in the presence of NEt_3 yielded the square-planar complex $[Pt(\mathbf{3_{ox\text{-}H}})_2]$ (**4**) (Scheme 7). Deprotonation of the PCHP moiety was performed in situ, by addition of the base together with the platinum complex and an excess of ligand. Compound **4** is remarkably stable and its purification takes advantage of its poor solubility in acetonitrile. An ORTEP view of its molecular structure in $\mathbf{4}{\cdot}4CH_2Cl_2$ is depicted in Figure 7.

In the planar, centrosymmetric structure of complex **4**, two molecules of deprotonated $\mathbf{3_{ox}}$ P,P-chelate the metal center with P−M−P angles of 70.42(2)°. The N1−C3 separation of 1.299(3) Å is consistent with a double bond character but

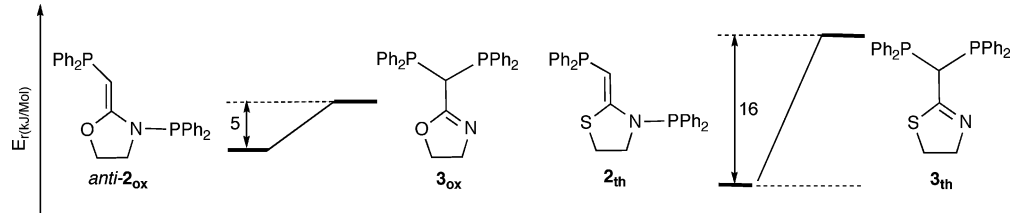

Figure 6. Relative energy diagrams for $\mathbf{2_{ox}}$, $\mathbf{3_{ox}}$ and $\mathbf{2_{th}}$, $\mathbf{3_{th}}$.

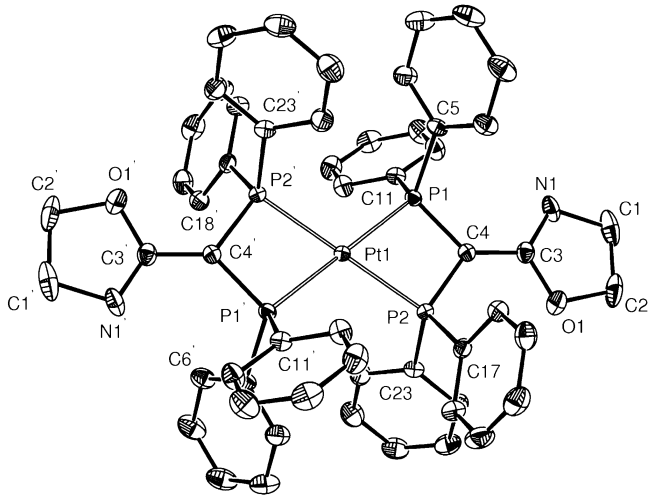

Figure 7. ORTEP view of the molecular structure of complex **4** in **4**·4CH_2Cl_2. Solvent molecules and hydrogen atoms omitted for clarity. Thermal ellipsoids are depicted at 50% level. Symmetry operation generating equivalent atoms (′): $-x$, $-y$, $-z$. Selected bond distances (Å) and angles (deg): Pt(1)−P(1), 2.3293(6); Pt(1)−P(2), 2.3164(6); P(1)−C(4), 1.745(3); P(2)−C(4), 1.751(2); C(3)−C(4), 1.432(3); N(1)−C(3), 1.299(3); O(1)−C(3), 1.356(3); P(1)−Pt(1)−P(2), 70.42(2); P(1)−Pt(1)−P(2)′, 109.58(2); P(1)−C(4)−P(2), 100.0(2); C(3)−C(4)−P(1), 130.8 (2); C(3)−C(4)−P(2), 129.0(2); C(4)−P(1)−Pt(1), 94.17(8); C(4)−P(2)−Pt(1), 94.46(9).

Scheme 8

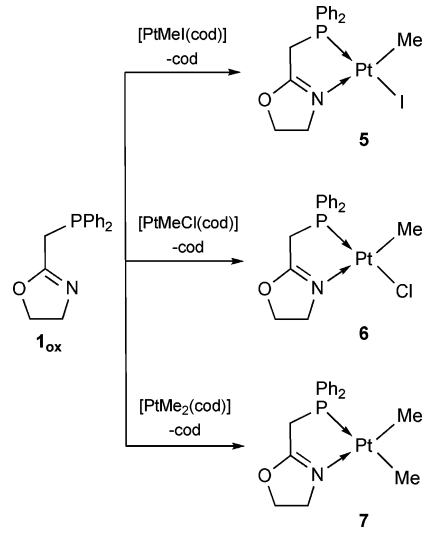

the P−C bond lengths [P1−C4, 1.745(3) Å; P2−C4, 1.751(2) Å], shorter than those typically found in tertiary phosphine complexes and the C3−C4 distance [1.432(3) Å] indicate that the double bond is delocalized over the P1, P2, C3, C4, N1 atoms, rather than solely over the C4−C3−N1 moiety. The geometry around the sp^2-hybridized C4 carbon atom is planar, the sum of the P−C−P and P−C−C angles being 359.69(2)°. These structural features are similar to those found in related metal complexes containing the chelating diphosphine obtained by deprotonation of $(Ph_2P)_2CHPy$ or its substituted analogues.[23a,25] N-functionalization on the oxazoline ring with other metal centers offers the potential to generate new heterometallic complexes, and this reactivity is currently under study.

The products of the reactions of ligand $\mathbf{1_{ox}}$ with [Pt(I)Me(cod)], [Pt(Cl)Me(cod)], and [$PtMe_2$(cod)] are reported in Scheme 8.

Single crystals of complexes **5** and **7** were obtained and studied by X-ray diffraction for comparative purpose. The ORTEP plots of their molecular structures are reported in Figures 8 and 9, respectively. Selected bond distances and angles are compared to those of **4** in Table 3.

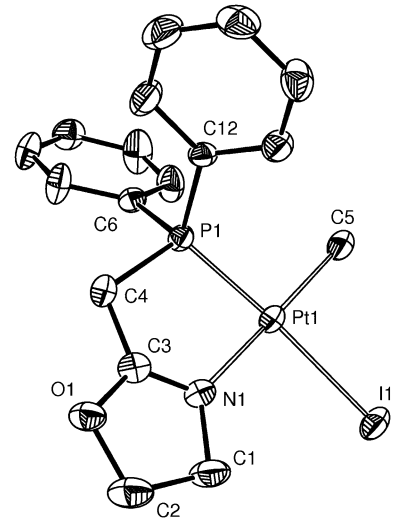

Figure 8. ORTEP plot of the molecular structure of compound **5**. H atoms omitted for clarity. Selected distances and angles are reported in Table 3. One of the two crystallographically independent molecules is depicted.

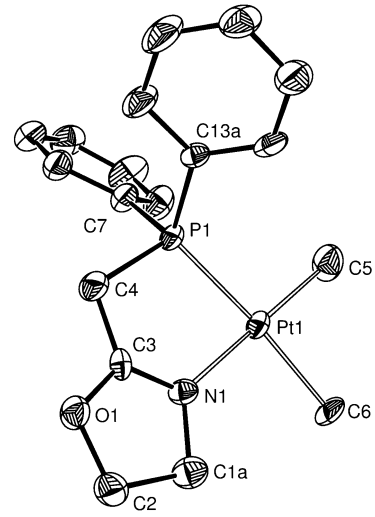

Figure 9. ORTEP plot of the molecular structure of compound **7**. H atoms omitted for clarity. Selected distances and angles are reported in Table 3. One of the two crystallographically independent molecules is depicted.

(21) For example, see: Imamura, Y.; Mizuta, T.; Miyoshi, K. *Organometallics* **2006**, *25*, 882–886.

(22) For recent examples, see: (a) Braun, L.; Liptau, P.; Kehr, G.; Ugolotti, J.; Froehlich, R.; Erker, G. *Dalton Trans.* **2007**, 1409–1415. (b) Piestert, F.; Fetouaki, R.; Bogza, M.; Oeser, T.; Blümel, J. *Chem. Commun.* **2005**, 1481–1483.

(23) (a) Mague, J. T.; Krinsky, J. L. *Inorg. Chem.* **2001**, *40*, 1962–1971. (b) Mague, J. T.; Hawbaker, S. W. *J. Chem. Crystallogr.* **1997**, *27*, 603−608; Mattson, B. M.; Ito, L. N. *Organometallics* **1989**, *8*, 391−395. (c) McNair, R. J.; Pignolet, L. H. *Inorg. Chem.* **1986**, *25*, 4717–4723. (d) Anderson, M. P.; Mattson, B. M.; Pignolet, L. H. *Inorg. Chem.* **1983**, *22*, 2644–2647. (e) Anderson, M. P.; Tso, C. C.; Mattson, B. M.; Pignolet, L. H. *Inorg. Chem.* **1983**, *22*, 3267–3275.

(24) Andrieu, J.; Braunstein, P.; Tiripicchio, A.; Ugozzoli, F. *Inorg. Chem.* **1996**, *35*, 5975–5985.

Table 3. Comparison between Selected Bond Distances (Å) and Angles (deg) in Compounds **4**·4CH_2Cl_2, **5**, and **7**[a]

	4·4CH_2Cl_2	**5**	**7**
Pt1−N1		2.128(5), 2.119(5)	2.111(7), 2.086(8)
Pt1−P1	2.3293(6)	2.192(2), 2.191(2)	2.258(2), 2.251(2)
Pt1−C5		2.095(6), 2.100(6)	2.042(9), 2.051(9)
Pt1−I1		2.6501(5), 2.6459(5)	
Pt1−C6			2.072(8), 2.161(9)
Pt1−Cl1			
N1−C3	1.299(3)	1.276(7), 1.284(8)	1.28(1), 1.29(1)
P1−C4	1.745(3)	1.858(6), 1.833(5)	1.862(9), 1.870(9)
C3−C4	1.432(3)	1.472(9), 1.480(8)	1.48(1), 1.51(1)
C3−O1	1.356(3)	1.346(7), 1.339(7)	1.338(9), 1.34(1)
C5−O2			
P1−Pt1−N1		83.5 (1), 82.2(1)	81.5(2), 83.2(2)
P1−Pt1−P2	70.42(2)		

[a] Two crystallographically independent molecules were present in the crystals of **5** and **7**.

Scheme 9

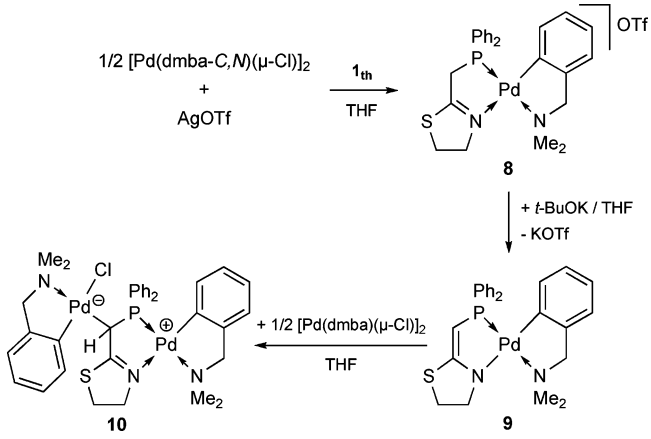

As expected, the phosphine $\mathbf{1_{ox}}$ chelates the metal center in complexes **5**−**7** through the P and N donor atoms. In **5**, the iodide and the methyl group are in trans position with respect to the phosphorus and nitrogen atoms, respectively, as observed in related complexes.[26] The ligand geometrical parameters remain almost the same in **5** and **7**, but the trans influence of the methyl group slightly elongates the Pt−P bond in **7**. Several crystal structures of variously substituted phosphino-methyl-oxazoline Pt and Pd complexes have been reported in the literature.[27] Since the bonding parameters of **5** and **7** are similar to those reported for other Pt(II) complexes bearing $\mathbf{1_{ox}}$,[27c] we shall not discuss them in detail, but their comparison with those for **4** is interesting and consistent with the delocalization of the double bond over the P1, P2, C3, C4, N1 atoms in the latter. The N1−C3 bond in **4** is only slightly longer than the corresponding bonds in **5** and **7**, while the P−C4 and C3−C4 bonds are significantly shorter. The P−Pt bonds of **4** are longer than those in **5** and **7**, as a result of the mutual trans influence of the phosphines and, probably, of the aforementioned electronic delocalization.

The reaction of $\mathbf{1_{th}}$ with the solvent-stabilized complex [Pd(dmba)$(THF)_n$]OTf prepared in situ (dmbaH = *N,N*-dimethylbenzylamine; OTf = CF_3SO_3) afforded [Pd(dmba-*C,N*)($\mathbf{1_{th}}$)]OTf (**8**) in almost quantitative yield. Complex **8** was deprotonated with *t*-BuOK to yield [Pd(dmba-*C,N*)($\mathbf{1_{th-H}}$)] (**9**) (Scheme 9). The deprotonation occurs selectively at the PCH_2 group of **8**, as indicated by ^{1}H NMR. The ^{31}P{^{1}H}

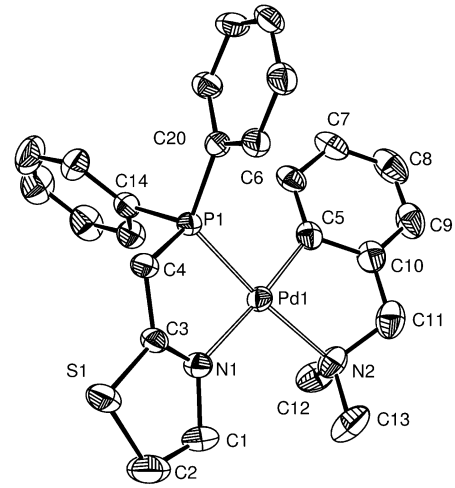

Figure 10. ORTEP plot of the molecular structure of the cation of compound **8** in **8**·0.25Et_2O. H atoms omitted for clarity. Selected distances and angles are reported in Table 4. One of the two crystallographic independent molecules is depicted.

Table 4. Comparison between Selected Bond Distances (Å) and Angles (deg) in Compounds **8** in **8**·0.25Et_2O, **9**, and **10** in **10**·2.5C_6H_6[a]

	8·0.25Et_2O	**9**	**10**·2.5C_6H_6
Pd1−N1	2.163(3), 2.154(3)	2.117(1)	2.140(2)
Pd1−P1	2.218(1), 2.228(1)	2.2410(5)	2.2299(7)
Pd1−C5	1.993(4), 2.002(4)	2.010(2)	2.006(3)
Pd1−N2	2.152(3), 2.154(3)	2.181(1)	2.162(2)
Pd2−C4			2.082(2)
Pd2−N3			2.150(2)
Pd2−C26			1.988(2)
Pd2−Cl1			2.4178(7)
N1−C3	1.273(5), 1.285(5)	1.330(2)	1.286(3)
P1−C4	1.834(4), 1.845(4)	1.749(2)	1.824(2)
C3−C4	1.478(5), 1.493(6)	1.375(2)	1.464(4)
C3−S1	1.747(4), 1.744(4)	1.780(2)	1.766(2)
P1−Pd1−N1	82.29(9), 79.61(9)	82.74(4)	81.01(6)
C5−Pd1−N2	82.5(2), 82.2(2)	81.43(6)	81.8(1)

[a] Two crystallographically independent molecules were present in the crystals of **8**.

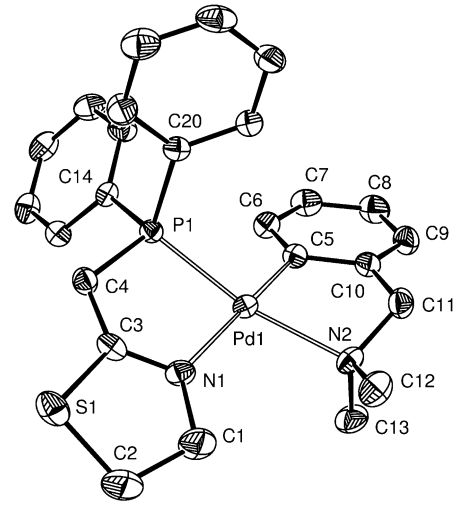

Figure 11. ORTEP plot of the molecular structure of compound **9.** H atoms omitted for clarity. Selected bond distances and angles are reported in Table 4.

(25) Mosquera, M. E. G.; Ruiz, J.; Garcia, G.; Marquinez, F. *Chem.*−*Eur. J.* **2006**, *12*, 7706–7716.

(26) (a) Agostinho, M.; Braunstein, P. *C. R. Chim.* **2007**, *10*, 666–676. (b) Agostinho, M.; Braunstein, P.; Welter, R. *Dalton Trans.* **2007**, 759–770.

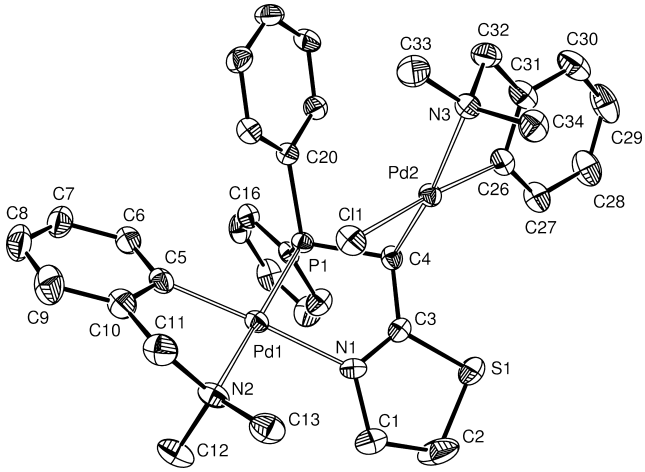

Figure 12. ORTEP plot of the molecular structure of the dinuclear complex **10** in **10**·2.5C_6H_6. H atoms omitted for clarity. Selected bond distances and angles are reported in Table 4.

NMR signal shifts from 45.8 (**8**) to 38.1 ppm (**9**). Both complexes were crystallized, and their molecular structures were determined by single crystal X-ray diffraction (Figures 10 and 11 and Table 4).

The ligand $\mathbf{1_{th}}$ chelates the metal center in **8** through the P and N atoms. A *C,N*-chelating dmba anion completes the metal coordination sphere. The chelation geometry is similar to that found for $\mathbf{1_{ox}}$, although the chelating five-membered ring of one of the two independent molecules is significantly less planar [P1−C4−C3−N1 torsion angle: 33.2(3)° (molecule B of **8**) compared, for example, to the 8.4(1)° torsion angle in molecule A of **5**]. The deprotonation results, as expected, in a shortening of the C3−C4 bond of **9** and in a slight elongation of the C3−S1 and C3−N1 bonds. The P1−C4 bond is also significantly shortened, similarly to what was encountered in **4**. A certain electronic delocalization is thus established over the P1−C4−C3−N1 moiety of **9**, in contrast to the more localized nature of the C═N double bond of **8**.

The nucleophilic sp^2 carbon atom C4 of **9** can regiospecifically attack further metal centers. Thus, reaction of **9** with [Pd(dmba-*C,N*)(μ-Cl)]$_2$ afforded [**9**·{Pd(dmba-*C,N*)Cl}] (**10**) (Scheme 9), of which the molecular structure was established by X-ray diffraction (Figure 12). Upon reaction, the C4 carbon becomes a stereogenic sp^3-hybridized center, and both enantiomers are present in the centrosymmetric unit cell, at variance with a similar complex bearing $\mathbf{1_{ox}}$.[27e]

In the dinuclear, zwitterionic complex **10**, the component **9** behaves as a metalloligand toward the fragment Pd(dmba-*C,N*)Cl through the carbon atom C4. The geometry around C4 is slightly distorted tetrahedral, the sum of the three angles involving C4, P1, C3, and Pd(2) being 328.4(2)°. The geometrical parameters of the P,N ligand are more similar to those of **8** than to those of **9** (for example, C3−C4 for **10**, 1.464(4) Å vs 1.375(2) for **9** and an average of 1.485(5) Å for **8**). Complex **10** features strong similarities with the analogous compound obtained with $\mathbf{1_{ox}}$,[27e] and its formation extends the use of neutral, stable metal complexes with a ligand-centered nucleophilicity as building blocks in polynuclear chemistry.

Conclusion

The mild reaction conditions used for the preparation of ligands such as $\mathbf{1_{ox}}$ and $\mathbf{1_{th}}$ may be extended to other imines susceptible to tautomerisation. The study of their formation and isomerization mechanisms suggests that the phosphoryl migrations reported herein could be more frequent than originally anticipated, since we observed similar reactivities in *alkyl*-phosphine (as $\mathbf{1_{ox)}}$ and *amino*-phosphine systems (such as diphenylphosphino-2-amino-2-thiazoline). Subtle but sometimes significant differences were observed between the oxazoline and thiazoline-based systems. Moreover, complex **4** represents a new example of functionalized metalloligand. Its reactivity toward further metal centers is under study, with promising preliminary results.

Acknowledgment. Support from the Centre National de la Recherche Scientifique, the Ministère de l'Enseignement Supérieur et de la Recherche, the French Embassy in Berlin, the DFG (Bonn), and the European Commission (Marie Curie fellowship HPMF-CT-2002-01659 and COST D-17 Action) is gratefully acknowledged. We thank Dr. A. DeCian (ULP Strasbourg) for the crystal structure data collection and Prof. R. Welter (ULP Strasbourg) for the refinement of the crystal structures of compounds **5**, **7**, **8**, **9**, and **10**.

Supporting Information Available: Listings of output Cartesian coordinates of the DFT calculations. This material is available free of charge via the Internet at http://pubs.acs.org.

IC800934H

(27) (a) Agostinho, M.; Braunstein, P. *Chem. Commun.* **2007**, 58–60. (b) Danjo, H.; Higuchi, M.; Yada, M.; Imamoto, T. *Tetrahedron Lett.* **2004**, *45*, 603–606. (c) Oberbeckmann-Winter, N.; Braunstein, P.; Welter, R. *Organometallics* **2004**, *23*, 6311–6318. (d) Thoumazet, C.; Melaimi, M.; Ricard, L.; Le Floch, P. *C. R. Chim.* **2004**, *7*, 823–832. (e) Apfelbacher, A.; Braunstein, P.; Brissieux, L.; Welter, R. *Dalton Trans.* **2003**, 1669–1674.